LBNL-43565
Preprint

ERNEST ORLANDO LAWRENCE
BERKELEY NATIONAL LABORATORY

Fast Poisson, Fast Helmholtz and Fast Linear Elastostatic Solvers on Rectangular Parallelepipeds

Andreas Wiegmann

Computing Sciences Directorate
Mathematics Department

June 1999

To be submitted
for publication

LBNL-43565

Fast Poisson, Fast Helmholtz and Fast Linear Elastostatic Solvers on Rectangular Parallelepipeds

Andreas Wiegmann

Computing Sciences Directorate
Department of Mathematics
Ernest Orlando Lawrence Berkeley National Laboratory
University of California
Berkeley, California 94720

June 1999

This work was supported by the Office of Science, Office of Advanced Scientific Computing Research, Mathematical, Information and Computational Science Division, Applied Mathematical Sciences Subprogram, of the U.S. Department of Energy under Contract No. DE-AC03-76SF00098.

Abstract

FFT–based fast Poisson and fast Helmholtz solvers on rectangular parallelepipeds for periodic boundary conditions in one-, two and three space dimensions can also be used to solve Dirichlet and Neumann boundary value problems. For non-zero boundary conditions, this is the special, grid–aligned case of jump corrections used in the Explicit Jump Immersed Interface method.

Fast elastostatic solvers for periodic boundary conditions in two and three dimensions can also be based on the FFT. From the periodic solvers we derive fast solvers for the new "normal" boundary conditions and essential boundary conditions on rectangular parallelepipeds. The periodic case allows a simple proof of existence and uniqueness of the solutions to the discretization of normal boundary conditions. Numerical examples demonstrate the efficiency of the fast elastostatic solvers for non–periodic boundary conditions.

More importantly, the fast solvers on rectangular parallelepipeds can be used together with the Immersed Interface Method to solve problems on non–rectangular domains with general boundary conditions. Details of this are reported in the preprint *The Explicit Jump Immersed Interface Method for 2D Linear Elastostatics* by the author.

Keywords: Fast Helmholtz solver, fast Poisson solver, fast elastostatic solver, boundary conditions.

1 Introduction

We derive fast solvers for the finite difference discretization of the equations of homogeneous linear elastostatics, also known as homogeneous small displacement elastostatics. We consider the approximation of plane stress or plane strain,

$$\begin{aligned} c\Delta u + \partial_{xx}u + \partial_{xy}v &= f^u, \\ c\Delta v + \partial_{yy}v + \partial_{xy}u &= f^v, \end{aligned} \tag{1}$$

as well as the discretization of the equations of homogeneous linear elastostatics in three dimensions

$$\begin{aligned} c\Delta u + \partial_{xx}u + \partial_{xy}v + \partial_{xz}w &= f^u, \\ c\Delta v + \partial_{yy}v + \partial_{yx}u + \partial_{yz}w &= f^v, \\ c\Delta w + \partial_{zz}w + \partial_{zx}u + \partial_{zy}v &= f^w, \end{aligned} \tag{2}$$

on rectangular parallelepipeds. The fast elastostatic solvers can be used in an embedding approach to solve elastostatic problems with traction, displacement and other boundary conditions on multiply connected, non–rectangular domains, which is the application of Schur–complement methods for Poisson problems on irregular domains by Buzbee, Dorr, George and Golub[1] and Proskurowski and Widlund [2] to the elastostatic equations. The main benefit of this approach is that it avoids mesh generation while allowing us to rapidly solve finely discretized problems in arbitrary domains in [7].

To introduce the notion of FFT–based fast solvers and our treatment of boundary conditions, we first consider discretizations of

$$(-\Delta + \kappa)\, u = -\sum_{i=1}^{M} \frac{\partial^2 u}{\partial x_i^2} + \kappa u = f, \quad (M = 1, 2, 3), \tag{3}$$

i.e. the Poisson equation ($\kappa = 0$) and the Helmholtz equation ($\kappa > 0$), with **periodic, Dirichlet** or **Neumann boundary conditions**.

We then write fast solvers for the elastostatic equations with **periodic** and **"normal" boundary conditions** and a somewhat slower approach for pure displacement (essential) boundary conditions.

For the purpose of exposition, all equations are approximated by a second order centered difference discretization with equidistant mesh ($\Delta x = h_1 = h$, $\Delta y = h_2$, $\Delta z = h_3$) in one, two or three space dimensions, i.e. on $[0, h_1 N_1]$, $[0, h_1 N_1] \times [0, h_2 N_2]$ or $[0, h_1 N_1] \times [0, h_2 N_2] \times [0, h_3 N_3]$, where $N_i \in \mathbf{N}$ and $h_i > 0$. But the derivation of the solvers is not limited to second order discretizations.

The basic idea is to find discrete analogies of solving differential equations via Fourier transforms. Recall that for $x \in \mathbf{R}^n$, $u : \mathbf{R}^n \to \mathbf{R}$ and $\mathcal{F}$ the n–dimensional Fourier Transform, we have

$$\mathcal{F}\left(\frac{\partial u}{\partial x_1}\right) = i\xi_1 \mathcal{F}(u), \qquad \mathcal{F}\left(\frac{\partial^2 u}{\partial x_2 \partial x_3}\right) = -\xi_2 \xi_3 \mathcal{F}(u), \quad \text{etc.}$$

Thus, the Helmholtz equation

$$-\Delta u + \kappa u = f$$

becomes

$$\left(\sum \xi_l^2 + \kappa\right) \mathcal{F}(u) = \mathcal{F}(f)$$

in Fourier space, where it is solved easily as

$$u = \mathcal{F}^{-1}\left(\frac{\mathcal{F}(f)}{\sum_{l=1}^{n} \xi_l^2 + \kappa}\right). \tag{4}$$

In the discrete case, it turns out one can replace $\mathcal{F}$ by the discrete Fourier transform (DFT); the work lies then in finding the appropriate divisors in the discrete equivalents of (4)—they depend on the discretization and boundary conditions—and dealing properly with the case $\kappa = 0$. Dirichlet and Neumann boundary conditions can be reduced to the periodic case.

In §2 we describe an approach that uses DFTs to solve the periodic Poisson and Helmholtz problems in $\mathcal{O}(N \ln N)$, where $N = N_1 N_2 N_3$. The ideas can be found for example in Schwarztrauber [4], but go back much further, see the references in [4], e.g. [1, 2]. The solution of the Poisson problem ($\kappa = 0$) with periodic boundary conditions exists only for f with $\int f = 0$ and in this case is unique only up to constants. Since these properties are inherited also by the discretized problem, we choose the solution to lie in the subspace $\mathcal{S}$ of grid functions whose entries sum to zero. This choice is natural as $\mathcal{S}$ is both the range and the orthogonal complement to the Nullspace of the (symmetric) discretization Δ_h^p of the Laplacian with periodic boundary conditions, so that Δ_h^p is invertible on $\mathcal{S}$.

Using tables of sines and cosines, it is easy to write fast sine–transform and fast cosine–transform based algorithms for the Neumann (§3) and Dirichlet (§4) problems (see also [4]). Because we had available a very efficient DFT (the FFT), but no comparable DCT or DST, we instead obtain solutions for Neumann and Dirichlet boundary conditions using the periodic solution on a larger domain which is results from reflection in each dimension.

The reflection approach deals naturally with the Nullspace of the discretization of the Neumann problem. For the Neumann problem with Schwarztrauber's discretization of the boundary conditions, the Nullspace of the discretization is also $\mathcal{S}$, but the range consists of vectors that sum to zero under a convention that boundary points on the relative interior carry half the weight of interior points. Corners in 2D and edges in 3D carry a quarter of the weight of interior points and corners in 3D carry an eighth of the weight of interior points. This is consistent with the reflection approach, where boundary points are duplicated differently from interior points, and depending on their position on the boundary.

The main points of this paper are in §5. There we consider the linear elastostatic equations for **periodic** boundary conditions in the approximation of plane stress (§5.1) and in 3D (§5.2). We describe fast solvers for what we will call **normal** boundary conditions in 2D (§5.3) and in 3D (§5.4). Normal boundary conditions mean given normal displacement and normal derivative of the tangential displacement. Our treatment of pure **Dirichlet** (displacement) boundary conditions in §5.5 avoids enlarging the domain at the cost of several fast solves, and shows how to deal with the "inverse" of the singular submatrix that arises when Dirichlet boundary conditions are treated via Schur–complement as a perturbation of periodic boundary conditions.

The fast solvers for second order centered finite difference approximations are shown to be useful also for non-rectangular regions in[7], and may turn out useful as preconditioners for homogenization approaches to structural topology design or as fast transform subdomain perconditioners in domain decomposition approaches.

2 Fast Poisson and Helmholtz solvers for periodic boundary conditions

Here we describe the use of FFTs for the fast inversion of the linear systems of equations resulting from the discretization of the Laplacian with periodic boundary conditions by centered second order differences. Upper case variable names indicate one-dimensional Fourier transforms, bars and hats mean Fourier transforms in the first two and all three variables, respectively. Due to periodicity, all arithmetic on the indices is modulo N_1, N_2 and N_3 in the first, second and third variables, respectively. The moduli are calculated as if we let the indices range from 0 to $N_j - 1$ instead of 1 to N_j. We use 1 to N_j for closer correspondence with our implementation — the programming language does not allow the index 0. Throughout we write $i = \sqrt{-1}$.

2.1 One space dimension

Discrete Fourier Transform (DFT):

$$U_k = \sum_{n=1}^{N_1} u_n \exp\left(\frac{-2\pi i(k-1)(n-1)}{N_1}\right) \qquad 1 \le k \le N_1.$$

Inverse DFT:

$$u_n = \frac{1}{N_1}\sum_{k=1}^{N_1} U_k \exp\left(\frac{2\pi i(k-1)(n-1)}{N_1}\right) \qquad 1 \le n \le N_1,$$

also

$$f_n = \frac{1}{N_1}\sum_{k=1}^{N_1} h_1^2 F_k \exp\left(\frac{2\pi i(k-1)(n-1)}{N_1}\right) \qquad 1 \le n \le N_1. \tag{5}$$

Finite differences for (3):

$$f_n = \frac{u_{n+1}}{h_1^2} - (\frac{2}{h_1^2} + \kappa)u_n + \frac{u_{n-1}}{h_1^2} =$$
$$\frac{1}{h_1^2 N_1}\sum_{k=1}^{N_1} U_k \exp\left(\frac{2\pi i(k-1)(n-1)}{N_1}\right)\left\{\exp\frac{2\pi(k-1)}{N_1} - 2 - h_1^2\kappa + \exp\frac{-2\pi(k-1)}{N_1}\right\} =$$
$$\frac{1}{h_1^2 N_1}\sum_{k=1}^{N_1} U_k \left\{2\cos\left(\frac{2\pi(k-1)}{N_1}\right) - 2 - h_1^2\kappa\right\}\exp\left(\frac{2\pi i(k-1)(n-1)}{N_1}\right).$$

Comparing coefficients of this Fourier series with the one in (5), we find

$$\left\{2\cos\left(\frac{2\pi(k-1)}{N_1}\right) - 2 - h_1^2\kappa\right\} U_k = h_1^2 F_k.$$

The left hand side is zero for $k = 1$ in case of the Poisson problem. In order for a solution to exist, we need $F_1 = 0$, which means simply $\sum f_n = 0$. In this case, we set $U_1 = 0$. For $2 \le k \le N_1$, ($1 \le k \le N_1$ for $\kappa > 0$) let

$$U_k = \frac{h_1^2 F_k}{2\cos\left(\frac{2\pi(k-1)}{N_1}\right) - 2 - h_1^2\kappa}. \tag{6}$$

Finally, recover u_n via inverse DFT. For $\kappa = 0$ the choice $U_1 = 0$ ensures $\sum_n u_n = 0$.

2.2 Two space dimensions

Now we use

$$f_{n,j} = \frac{u_{n+1,j}}{h_1^2} + \frac{u_{n,j+1}}{h_2^2} - (\frac{2}{h_1^2} + \frac{2}{h_2^2} + \kappa)u_{n,j} + \frac{u_{n-1,j}}{h_1^2} + \frac{u_{n,j-1}}{h_2^2} =$$
$$\frac{1}{h_1^2 h_2^2 N_1}\sum_{k=1}^{N_1} U_{k,j} \exp\left(\frac{2\pi i(k-1)(n-1)}{N_1}\right)\left\{2h_2^2\cos\left(\frac{2\pi(k-1)}{N_1}\right) - 2h_1^2 - 2h_2^2 - h_1^2 h_2^2\kappa\right\} +$$
$$+ \frac{1}{h_2^2 N_1}\sum_{k=1}^{N_1} U_{k,j+1}\exp\left(\frac{2\pi i(k-1)(n-1)}{N_1}\right) + \frac{1}{h_2^2 N_1}\sum_{k=1}^{N_1} U_{k,j-1}\exp\left(\frac{2\pi i(k-1)(n-1)}{N_1}\right).$$

This decouples into N_1 periodically tridiagonal linear systems indexed by $k = 1, 2, \ldots N_1$. For fixed k, the system is given by

$$\frac{U_{k,j+1}}{h_2^2} + \left\{\frac{\cos\left(\frac{2\pi(k-1)}{N_1}\right) - 2}{h_1^2} - \frac{2}{h_2^2} - \kappa\right\} U_{k,j} + \frac{U_{k,j-1}}{h_2^2} = F_{k,j}, \text{ for } j = 1, 2, \ldots, N_2. \tag{7}$$

We could continue with a Fourier transform in the second variable. This idea is described for the 3D case in the next section. Alternatively, one can solve the periodically tridiagonal system (7) for each k. Due to the special structure of the matrices, this is possible in $\mathcal{O}(N_2)$. For $\kappa = 0$ and $k = 1$, the matrix is rank deficient—it is simply the one dimensional periodic centered difference operator considered in §2.1. Right hand sides with sum zero are in the range of this matrix. In that case, we set $U_{1,1} = 0$ and solve the $(N_1 - 1) \times (N_1 - 1)$ system which is obtained from (7) by scratching the first row and first column for $U_{i,1}$, for $i = 2, 3, \ldots, N_2$. Finally, N_1 inverse FFTs of length N_2 give u. As in §2.1, for $\kappa = 0$ the choice of $U_{1,1} = 0$ ensures that $u \in \mathcal{S}$.

2.3 Three space dimensions

We do a DFT on the first index, and find (for fixed n)

$$f_{n,j,l} = \frac{u_{n+1,j,l}}{h_1^2} + \frac{u_{n,j+1,l}}{h_2^2} + \frac{u_{n,j,l+1}}{h_3^2} - \left(\frac{2}{h_1^2} + \frac{2}{h_2^2} + \frac{2}{h_3^2} + \kappa\right) u_{n,j,l} + \frac{u_{n-1,j,l}}{h_1^2} + \frac{u_{n,j-1,l}}{h_2^2} + \frac{u_{n,j,l-1}}{h_3^2} =$$

$$\frac{1}{N_1}\sum_{k=1}^{N_1} U_{k,j,l} \exp\left(\frac{2\pi i(k-1)(n-1)}{N_1}\right) \left\{\frac{2\cos\left(\frac{2\pi(k-1)}{N_1}\right) - 2}{h_1^2} - \frac{2}{h_2^2} - \frac{2}{h_3^2} - \kappa\right\} +$$

$$+ \frac{1}{h_2^2 N_1}\sum_{k=1}^{N_1} U(k,j+1,l) \exp\left(\frac{2\pi i(k-1)(n-1)}{N_1}\right) + \frac{1}{h_2^2 N_1}\sum_{k=1}^{N_1} U_{k,j-1,l} \exp\left(\frac{2\pi i(k-1)(n-1)}{N_1}\right) +$$

$$+ \frac{1}{h_3^2 N_1}\sum_{k=1}^{N_1} U_{k,j,l+1} \exp\left(\frac{2\pi i(k-1)(n-1)}{N_1}\right) + \frac{1}{h_3^2 N_1}\sum_{k=1}^{N_1} U_{k,j,l-1} \exp\left(\frac{2\pi i(k-1)(n-1)}{N_1}\right).$$

Comparing Fourier coefficients,

$$\frac{U_{k,j+1,l}}{h_2^2} + \frac{U_{k,j,l+1}}{h_3^2} + \left\{\frac{2\cos\left(\frac{2\pi(k-1)}{N_1}\right) - 2}{h_1^2} - \frac{2}{h_2^2} - \frac{2}{h_3^2} - \kappa\right\} U_{k,j,l} + \frac{U_{k,j-1,l}}{h_2^2} + \frac{U_{k,j,l-1}}{h_3^2} = F_{k,j,l}.$$

Denoting the variables transformed in the first two indices by bars, we get (for fixed k)

$$\frac{U_{k,j+1,l}}{h_2^2} + \frac{U_{k,j,l+1}}{h_3^2} + \left\{\frac{2\cos\left(\frac{2\pi(k-1)}{N_1}\right) - 2}{h_1^2} - \frac{2}{h_2^2} - \frac{2}{h_3^2} - \kappa\right\} U_{k,j,l} + \frac{U_{k,j-1,l}}{h_2^2} + \frac{U_{k,j,l-1}}{h_3^2} =$$

$$\frac{1}{N_2}\sum_{m=1}^{N_2} \bar{U}_{k,m,l} \exp\left(\frac{2\pi(m-1)(k-1)}{N_2}\right) \left\{\frac{2\cos\left(\frac{2\pi(k-1)}{N_1}\right) - 2}{h_1^2} - \frac{2\cos\left(\frac{2\pi(m-1)}{N_2}\right) - 2}{h_2^2} - \frac{2}{h_3^2} - \kappa\right\} +$$

$$+ \frac{1}{h_3^2 N_2}\sum_{m=1}^{N_2} \bar{U}_{k,m,l+1} \exp\left(\frac{2\pi i(m-1)(k-1)}{N_2}\right) + \frac{1}{h_3^2 N_2}\sum_{m=1}^{N_2} \bar{U}_{k,m,l-1} \exp\left(\frac{2\pi i(m-1)(k-1)}{N_2}\right).$$

Thus we get $N_1 N_2$ tridiagonal systems, indexed by $k = 1, 2, \ldots N_1$, $m = 1, 2, \ldots, N_2$,

$$\frac{\bar{U}_{k,m,l+1}}{h_3^2} + \left\{\frac{2\cos\left(\frac{2\pi(k-1)}{N_1}\right) - 2}{h_1^2} + \frac{2\cos\left(\frac{2\pi(m-1)}{N_2}\right) - 2}{h_2^2} - \frac{2}{h_3^2} - \kappa\right\} \bar{U}_{k,m,l} + \frac{\bar{U}_{k,m,l-1}}{h_3^2} = \bar{F}_{k,m,l}.$$

These tridiagonal systems can be solved as before, but clearly another DFT (in the third variable, denoted by hats) reduces this to

$$\left\{\frac{2\cos\left(\frac{2\pi(k-1)}{N_1}\right) - 2}{h_1^2} + \frac{2\cos\left(\frac{2\pi(m-1)}{N_2}\right) - 2}{h_2^2} + \frac{2\cos\left(\frac{2\pi(p-1)}{N_3}\right) - 2}{h_3^2} - \kappa\right\} \hat{U}_{k,m,p} = \hat{F}_{k,m,p}.$$

The left hand factor is zero for $\kappa = 0$ and $k = m = p = 1$, so that we need to require $\hat{F}(1,1,1) = 0$ and set $\hat{U}(1,1,1) = 0$ just as in the one dimensional case. Otherwise, for $(k,m,p) \neq (1,1,1)$ (any (k,m,p) if $\kappa > 0$),

$$\hat{U}_{k,m,p} = \frac{\hat{F}_{k,m,p}}{\frac{2\cos\left(\frac{2\pi(k-1)}{N_1}\right)-2}{h_1^2} + \frac{2\cos\left(\frac{2\pi(m-1)}{N_2}\right)-2}{h_2^2} + \frac{2\cos\left(\frac{2\pi(p-1)}{N_3}\right)-2}{h_3^2} - \kappa}. \tag{8}$$

Finally, $N_1 N_2$ inverse DFTs of length N_3, $N_1 N_3$ inverse DFTs of length N_2 and $N_2 N_3$ inverse DFTs of length N_1 give the answer, $u_{n,j,l}$. As in §2.1, for $\kappa = 0$ the choice of $U_{1,1,1} = 0$ ensures that $u \in \mathcal{S}$.

Remark 2.1

- *Equations (6) and (8) are the discrete analogies of (4) in 1D and 3D, respectively.*
- *For clarity of exposition, we have assumed that each DFT is one-dimensional in nature. Of course the formulas can also be used with two– and three–dimensional DFTs.*
- *We assume that a Fast Fourier Transform will be used, and hence the procedure works fastest if N_1, N_2 and N_3 are powers of 2.*
- *It is clear how to generalize to fast poisson solvers in N dimensions for $N \geq 4$.*

3 Poisson and Helmholtz equations with Neumann boundary conditions

3.1 One space dimension

Recall that in one space dimension, we write $\Delta x = h$ for h_1. Schwarztrauber [4] discretizes the Poisson Problem with centered differences and Neumann boundary conditions using ghost values

$$u_{-1} = u_1,$$
$$u_{N_1+1} = u_{N_1-1}.$$

The ghost values are used to modify the standard centered differences for the boundary points.

$$2u_1 - 2u_0 = h^2 f_0,$$
$$2u_{N_1-1} - 2u_{N_1} = h^2 f_{N_1}.$$

This discretization of Neumann boundary conditions is characterized by the following features

- The boundary is grid aligned.
- The equation holds and f is known all the way up to including the boundary.
- Using the fictitious point, the standard second order centered discretization of the differential equation can be used on the boundary.
- The second order centered discretization of the Neumann boundary condition is also written using the fictitious point.
- Between these two equations, the solution value at the fictitious point is eliminated, resulting in a combined equation for the boundary value instead of the discretization of the boundary condition and the discretization of the differential equation.
- In 1D, the resulting tridiagonal system is solved directly, in 2D a tridiagonal system is created by making an Ansatz in a Cosine series, as in §3.4.

We proceed similarly, but wish to find solutions in an exponential series, in order to use the DFT. Schwarztrauber's discretization results in a singular matrix, with kernel consisting of the constant vectors, and the range consisting of all vectors whose weighted sum is zero. Endpoints in 1D as well as interior side points in 2D and 3D carry the weight 1/2 in the summation, corners in 2D and edges in 3D carry the weight 1/4 and corners in 3D carry the weight 1/8.

Suppose $\mathbf{u} = [u_0, u_1, \ldots, u_{N_1}]^T$ consists of values of a solution at the left boundary, at the interior grid points and at the right boundary, in this order, for some right hand side $\mathbf{f} = [f_0, f_1, \ldots, f_{N_1-1}, f_{N_1}]^T$ that satisfies the weighted sum condition.

Theorem 1 *The solution of the periodic problem on $2N_1$ grid points with right hand side*

$$\tilde{\mathbf{f}} = [f_0, f_1, \dots, f_{N_1-1}, f_{N_1}, f_{N_1-1}, \dots, f_1], \tag{9}$$

is

$$\tilde{\mathbf{u}} = [u_0, u_1, \dots, u_{N_1-1}, u_{N_1}, u_{N_1-1}, \dots, u_1], \tag{10}$$

where $u_0 = -h^2 f_0/2 - u_1$ and $u_N = -h^2 f_{N_1}/2 - u_{N_1-1}$

Proof. The symmetric continuations of $\mathbf{u}$ and $\mathbf{f}$ satisfy the periodic equations (index arithmetic modulo $2N_1 - 1$) on the enlarged domain

$$\tilde{u}_{n+1} - 2\tilde{u}_n + \tilde{u}_{n-1} = h^2 \tilde{f}_n \text{ for } n = 0, 1, 2, \dots, 2N_1 - 1, \tag{11}$$

and also the centered discretizations of the Neumann boundary conditions,

$$\tilde{u}_1 - \tilde{u}_{-1} = \tilde{u}_1 - \tilde{u}_{2N_1-1} = 0,$$
$$\tilde{u}_{N_1+1} - \tilde{u}_{N_1-1} = 0.$$

□

The weighted sum condition on $\mathbf{f}$ ensures that $\tilde{\mathbf{f}}$ lies in the range of the periodic operator, the Neumann boundary value problem is reduced to the methods of the previous section for both the Laplace and Helmholtz operator.

3.2 Non–zero Neumann data

Now consider non-vanishing Neumann data, $u_x(0) = b_0$ and $u_x(N_1) = b_{N_1}$. These values appear in the discretization of the derivative,

$$u_1 - u_{-1} = 2hb_0,$$
$$u_{N_1+1} - u_{N_1-1} = 2hb_{N_1},$$

and thus as sources in the combined equation. The solution $\tilde{\mathbf{u}}$ tends to a continuous, but not differentiable function as the grid is refined. Schwarztrauber's values at the fictitious points **do not agree** with our symmetric extension (10) , but are instead "corrected" by jumps in the first derivative of the magnitude of the Neumann boundary value. So (11) for $n = 0, N_1$ becomes

$$\tilde{u}_1 - 2\tilde{u}_0 + \tilde{u}_{2N_1-1} = h^2 \tilde{f}_0 - h[u_x]_{0-} - h[u_x]_{0+}, \tag{12}$$
$$\tilde{u}_{N_1+1} - 2\tilde{u}_{N_1} + \tilde{u}_{N_1-1} = h^2 \tilde{f}_{N_1} - h[u_x]_{(N_1)-} - h[u_x]_{(N_1)+}, \tag{13}$$

where $[u_x]_{0-} = [u_x]_{0+} = b_0$ and $[u_x]_{(N_1)-} = [u_x]_{(N_1)+} = -b_{N_1}$.

The factor h in the corrections results from the fact that the jump occurs exactly at the grid point; this is also the reason why each jump is needed to correct only a single equation. In the other equations corrected by the jumps, the corresponding factor is zero. More explicitly comparing with the Explicit Jump Immersed Interface Method (c.f. [9, equations (5) and (6)]), (11) for $n = 1, N_1 - 1, N_1 + 1, 2N_1 - 1$ results from

$$\tilde{u}_2 - 2\tilde{u}_1 + \tilde{u}_0 = h^2 \tilde{f}_1 - 0[u_x]_{0+},$$
$$\tilde{u}_0 - 2\tilde{u}_{2N_1-1} + \tilde{u}_{2N_1-2} = h^2 \tilde{f}_{2N_1-1} - 0[u_x]_{0-},$$
$$\tilde{u}_{N_1+2} - 2\tilde{u}_{N_1+1} + \tilde{u}_{N_1} = h^2 \tilde{f}_{N_1+1} - 0[u_x]_{(N_1)+},$$
$$\tilde{u}_{N_1} - 2\tilde{u}_{N_1-1} + \tilde{u}_{N_1-2} = h^2 \tilde{f}_{N_1-1} - 0[u_x]_{(N_1)-}.$$

No second order corrections are needed due to the continuity of the extension of $\mathbf{f}$ to $\tilde{\mathbf{f}}$, i.e. $[u_{xx}] = 0$. A nonzero Neumann boundary condition yields an example of EJIIM corrections in the special case of a discrete single layer potential occurring at a boundary point.

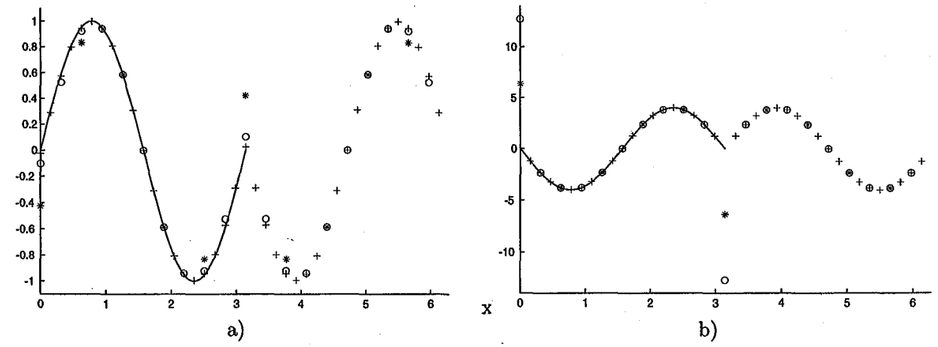

Figure 1: *The extended solutions $\tilde{u}$ in a) and right hand side $\tilde{f}$ in b), for $f(x) = -4\sin(2x)$ and $N = 5, 10, 20$ (stars, circles and crosses). As the grid is refined, the values of $\tilde{f}$ at 0 and π tend to ∞ in such a way that the kinks in $\tilde{u}$ remain the same. The Poisson solver fixes the constant c so that $\sum \tilde{u}_i = 0$. The discrete solution values converge rapidly to the exact solution (solid line).*

3.2.1 Example

The function $u(x) = \sin(2x) - c$ solves $u_{xx} = -4\sin(2x)$ with $u_x(0) = 1$ and $u_x(\pi) = 1$ for any c. The "singularity" of $\tilde{f}$ can be clearly seen in Figure 1 b). As the grid is refined, the values at $0(= 2\pi)$ and π tend to $\pm\infty$ in such a way that the kinks in $\tilde{u}$ remain the same. The Poisson solver fixes the constant c so that $\sum \tilde{u}_i = 0$.

3.3 Higher dimensional issues

The extension to d space dimensions for the periodic solver as well as non–zero Neumann boundary conditions is straight forward. The reorderings of the extensions are indicated symbolically below. The letter f and its reflections (typewritten letters mean that the third index is reflected) indicate the d–dimensional array of interior grid values. Solid lines mean appropriate boundary values for f are filled in.

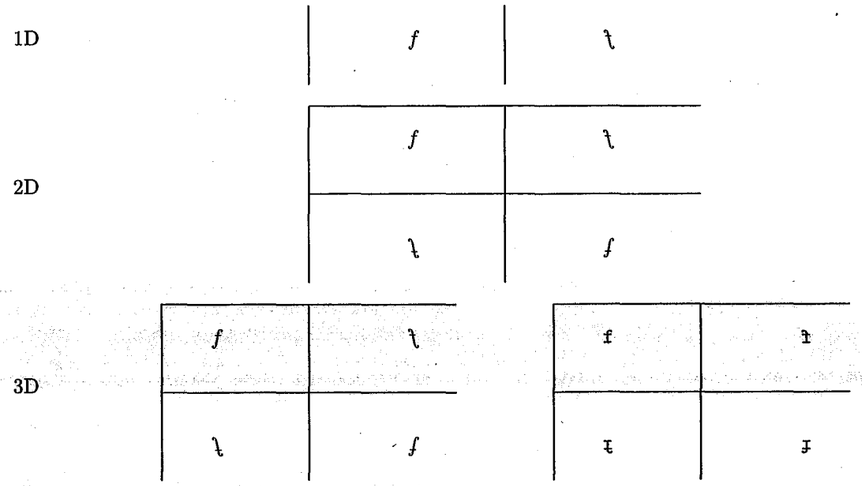

In 3D, there is also a layer of boundary values below the left and between the two 3D arrays.

The reflection ansatz has the drawback that the size of the problem is increased like 2^d. Schwarztrauber [4] and §3.4 shows how an ansatz in sine series can avoid this growth. However, for clarity of exposition, for analogy with the elastostatic case, to observe connections with the Immersed Interface Method mentioned in [7], and because we have a fast DFT but no fast discrete sine transform in Matlab, we prefer the ansatz in exponential series.

3.4 Neumann boundary conditions solved on the original domain

Consider the one-dimensional problem with Schwarztrauber's discretization, i.e. with right hand side given at the left endpoint, f_0, at interior points, f_n, $n = 1, 2, \ldots, N-1$ and at the right endpoint, f_N. Recall the periodic transform on N points,

$$F_k = \sum_{n=1}^{N} f_n \exp\left(\frac{-2\pi i(k-1)(n-1)}{N}\right) \qquad 1 \le k \le N.$$

We use the indexing convention $\tilde{f}_1 = f_0$, $\tilde{f}_2 = f_1$, ..., $\tilde{f}_{N+1} = f_N$, $\tilde{f}_{N+2} = f_{N-1}$, ..., $\tilde{f}_{2N} = f_1$ and write out the transform on the periodically extended domain,

$$\tilde{F}_k = \sum_{n=1}^{2N} \tilde{f}_n \exp\left(\frac{-2\pi i(k-1)(n-1)}{2N}\right) \qquad 1 \le k \le 2N.$$

We observe that $\tilde{f}_n = \tilde{f}_{2N-n+2}$ for $2 \le n \le N$, and also

$$\exp\left(\frac{-2\pi i(k-1)(n-1)}{N}\right) + \exp\left(\frac{-2\pi i(k-1)(2N-n+2-1)}{N}\right) = 2\cos\left(\frac{2\pi(k-1)(n-1)}{N}\right),$$

$$\exp\left(\frac{-2\pi i(k-1)0}{N}\right) = 1,$$

$$\exp\left(\frac{-2\pi i(k-1)(N+1-1)}{N}\right) = (-1)^{(k-1)}.$$

Thus

$$\tilde{F}_k = \tilde{f}_1 + (-1)^{(k-1)}\tilde{f}_{N+1} + 2\sum_{n=2}^{N} \tilde{f}_n \cos\left(\frac{2\pi(k-1)(n-1)}{N}\right) \qquad 1 \le k \le 2N.$$

Finally, since

$$\cos\left(\frac{2\pi(k-1)(n-1)}{N}\right) = \cos\left(\frac{2\pi(k-1)(1-n)}{N}\right) = \cos\left(\frac{2\pi(2N-k+2-1)(n-1)}{N}\right)$$

and

$$(-1)^{(k-1)} = (-1)^{(2N-k+2-1)},$$

we also get

$$\tilde{F}_k = \tilde{F}_{2N-k+2} \qquad 1 \le k \le N.$$

Together with the symmetry of the denominators in (6), (7) and (8), the Neumann boundary problem can thus be solved on the original domain with cosine and inverse cosine transforms.

4 Poisson and Helmholtz equations with Dirichlet Boundary Conditions

4.1 One space dimension

To solve $u_{xx} = f$, with zero Dirichlet boundary conditions, observe that $u_{N_1} = 0$ and suppose that $\mathbf{u} = [u_1, u_2, \ldots, u_{N_1-1}]^T$ solves the discrete problem with zero Dirichlet boundary conditions (the matrix for the

Dirichlet problem is obtained from the periodic one by scratching the last row and column) and right hand side $\mathbf{f} = [f_1, f_2, \ldots, f_{N_1-1}]$.

Theorem 2 *The solution of the periodic problem on $2N_1$ grid points with right hand side*

$$\tilde{\mathbf{f}} = \{\tilde{f}_i\}_{i=0}^{2N-1} \equiv [0, f_1, f_2, \ldots, f_{N_1-1}, 0, -f_{N_1-1}, -f_{N_1-2}, \ldots, -f_1]^T$$

is

$$\tilde{\mathbf{u}} = \{\tilde{u}_i\}_{i=0}^{2N-1} \equiv [0, u_1, u_2, \ldots, u_{N_1-1}, 0, -u_{N_1-1}, -u_{N_1-2}, \ldots, -u_1]^T.$$

Proof. The equations clearly hold at interior grid points and we need to check only at the boundary points:

$$\frac{\tilde{u}_1 - 2\tilde{u}_0 + \tilde{u}_{2N-1}}{h^2} = 0$$

follows from $\tilde{u}_{2N-1} = -\tilde{u}_1$ and $\tilde{u}_0 = 0$.

$$\frac{\tilde{u}_{N+1} - 2\tilde{u}_N + \tilde{u}_{N-1}}{h^2} = 0$$

follows from $\tilde{u}_{N+1} = -\tilde{u}_{N-1}$ and $\tilde{u}_N = 0$. □

The compatibility condition for the periodic system is satisfied, i.e. $\sum \tilde{u}_i = \sum \tilde{f}_i = 0$, and again the problem is reduced to the methods of §2.

4.2 Non–zero Dirichlet data

For non-zero Dirichlet data, the boundary values are placed in $\mathbf{f}$ as usual, and the method works as it is. Denote the boundary values on the left and right by $\bar{u}_0$ and $\bar{u}_N$, respectively and use the second order singular right hand side. According to our convention from §2, $h = h_1$ and $N = N_1$.

$$\begin{aligned}
\tilde{f}_{N-1} &= f_{N-1} - \bar{u}_N/h^2, \\
\tilde{f}_{N+1} &= -f_{N-1} + \bar{u}_N/h^2, \\
\tilde{f}_1 &= f_1 - \bar{u}_0/h^2, \\
\tilde{f}_{2N-1} &= -f_1 + \bar{u}_0/h^2.
\end{aligned}$$

The solution $\tilde{\mathbf{f}}$ tends to a discontinuous function as the grid is refined. On the original boundary, $\tilde{\mathbf{u}}$ is zero, while quadratic extrapolation from interior points to the boundary results in the desired boundary values, and their negative on the other (extended) side. This is the discrete analogue of a double layer potential and the special case of two corrections in the EJIIM sense (c.f. [9, equations (5) and (6)]) occurring at each boundary gridpoint, infinitesimally close on the two sides:

$$\begin{aligned}
\tilde{f}_{N-1} &= f_{N-1} - [u]_{N^-}/h^2, \\
\tilde{f}_N &= 0 + [u]_{N^-}/h^2 - [u]_{N^+}/h^2, \\
\tilde{f}_{N+1} &= -f_{N-1} + [u]_{N^+}/h^2, \\
\tilde{f}_{2N-1} &= -f_1 + [u]_{0^-}/h^2, \\
\tilde{f}_0 &= 0 + [u]_{0^+}/h^2 - [u]_{0^-}/h^2, \\
\tilde{f}_1 &= f_1 - [u]_{0^+}/h^2.
\end{aligned}$$

4.2.1 Example

The function $u(x) = \cos(2x)$ solves $u_{xx} = -4\cos(2x)$ with $u(0) = 1$ and $u(\pi) = 1$. The "singularity" of $\tilde{f}$ can be clearly seen in Figure 2 b). As the grid is refined, the values at grid points just to the left and right of $0(= 2\pi)$ and π tend to $\pm\infty$ in such a way that the discontinuities in $\tilde{u}$ remain the same. Note that on all grids due to $\tilde{u}(0) = \tilde{u}(\pi) = 0$, the discretization "has four discontinuities".

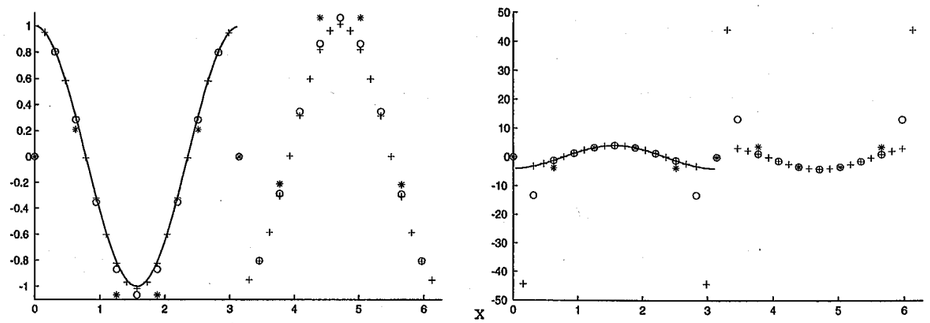

Figure 2: *The extended solutions $\tilde{u}$ in a) and right hand side $\tilde{f}$ in b), for $f(x) = -4\cos(2x)$ and $N = 5, 10, 20$ (stars, circles and crosses). As the grid is refined, the values of $\tilde{f}$ at grid points just to the left and right of $0(= 2\pi)$ and π tend to $\pm\infty$ in such a way that the discontinuities in $\tilde{u}$ remain the same. The discrete solution values converge rapidly to the exact solution (solid line).*

4.3 Higher dimensional issues

The extension to d space dimensions is clear. The reorderings of the extensions are indicated symbolically below. The letter f and its reflections (typewritten letters mean that the third index is reflected) indicate the d–dimensional array of interior grid values. Vertical solid lines indicate columns and horizontal lines indicate rows of zeros.

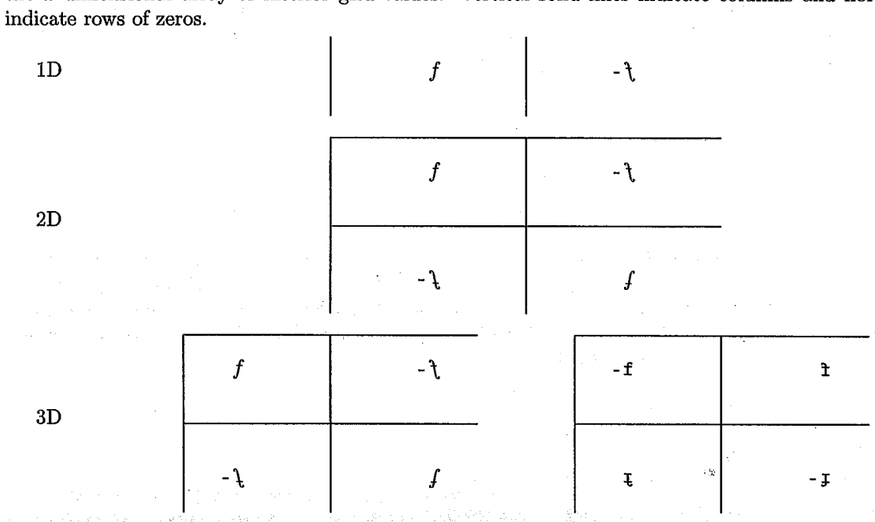

In 3D, there is also a layer of zeros below the left and between the two 3D arrays.

4.4 Dirichlet boundary conditions solved on the original domain

Consider the one-dimensional problem with right hand side given at the interior points, f_n, $n = 1, 2, \ldots, N-1$, and antisymmetric extension by zeros on the boundaries and $-f$. Recall the periodic transform on N points,

$$F_k = \sum_{n=1}^{N} f_n \exp\left(\frac{-2\pi i(k-1)(n-1)}{2N}\right) \quad 1 \le k \le N.$$

We use the indexing convention $\tilde{f}_1 = 0$, $\tilde{f}_2 = -f_1$, $\ldots$, $\tilde{f}_N = -f_{N-1}$, $\tilde{f}_{N+1} = 0$, $\tilde{f}_{N+2} = -f_{N-1}$, $\tilde{f}_{N+3} = -f_{N-2}$, $\ldots$, $\tilde{f}_{2N} = f_1$ and write out the transform on the periodically extended domain,

$$\tilde{F}_k = \sum_{n=1}^{2N} \tilde{f}_n \exp\left(\frac{-2\pi i(k-1)(n-1)}{2N}\right) \quad 1 \le k \le 2N.$$

We observe that $\tilde{f}_n = -\tilde{f}_{2N-n+2}$ for $2 \le n \le N$, and also

$$\exp\left(\frac{-2\pi i(k-1)(n-1)}{N}\right) - \exp\left(\frac{-2\pi i(k-1)(2N-n+2-1)}{N}\right) = 2i\sin\left(\frac{-2\pi(k-1)(n-1)}{N}\right).$$

Thus

$$\tilde{F}_k = 2i\sum_{n=2}^{N} \tilde{f}_n \sin\left(\frac{-2\pi(k-1)(n-1)}{N}\right) \quad 1 \le k \le 2N.$$

Finally, since

$$\sin\left(\frac{-2\pi(k-1)(n-1)}{N}\right) = -\sin\left(\frac{-2\pi(k-1)(1-n)}{N}\right) = -\sin\left(\frac{-2\pi(2N-k+2-1)(n-1)}{N}\right),$$

we also get

$$\tilde{F}_k = -\tilde{F}_{2N-k+2} \quad 1 \le k \le N.$$

Together with the symmetry of the denominators in (6), (7) and (8), the Dirichlet boundary problem can thus be solved on the original domain with sine and inverse sine transforms.

5 Fast elastostatic solvers on rectangular parallelepipeds

Throughout this section, Ω is the rectangle $[0, N_1 h] \times [0, N_2 h]$, where $h = \Delta x = \Delta y$ is the uniform meshwidth and N_1 and N_2 are numbers of grid points in a discretization with periodic boundary conditions. The equations are discretized by centered second ordered finite differences (see (14) and (15) below), Dirichlet and Neumann boundary conditions are imposed by finite differences as for Laplace's equation in §4 and §3.

5.1 Periodic boundary conditions in 2D

Consider the equidistant ($\Delta x = \Delta y = h$) discretization of

$$c\Delta u + \partial_{xx} u + \partial_{xy} v = f^u \text{ in } \Omega,$$
$$c\Delta v + \partial_{xy} u + \partial_{yy} v = f^v \text{ in } \Omega,$$

with u and v periodic. The boundaries $x = 0$ and $x = N_1 h$ are identified by periodicity as are the boundaries $y = 0$ and $y = N_2 h$. We write out second order finite differences in detail for the point (nh, jh).

$$cu_{n+1,j} + cu_{n,j+1} - 4cu_{n,j} + cu_{n-1,j} + cu_{n,j-1} + u_{n+1,j} - 2u_{n,j} + u_{n-1,j} + \\ + v_{n+1,j+1}/4 - v_{n-1,j+1}/4 - v_{n+1,j-1}/4 + v_{n-1,j-1}/4 = h^2 f^u_{n,j} \quad (14)$$

and

$$cv_{n+1,j} + cv_{n,j+1} - 4cv_{n,j} + cv_{n-1,j} + cv_{n,j-1} + v_{n,j+1} - 2v_{n,j} + v_{n,j-1} + \\ + u_{n+1,j+1}/4 - u_{n-1,j+1}/4 - u_{n+1,j-1}/4 + u_{n-1,j-1}/4 = h^2 f^v_{n,j}. \quad (15)$$

As before the discrete Fourier transform (DFT) in the first variable (recall that $i = \sqrt{-1}$) is indicated by upper case variables

$$U_{k,j} = \sum_{n=1}^{N_1} u_{n,j} \exp\left(\frac{-2\pi i(k-1)(n-1)}{N_1}\right) \quad 1 \le k \le N_1,$$

and the inverse DFT is

$$u_{n,j} = \frac{1}{N_1} \sum_{k=1}^{N_1} U_{k,j} \exp\left(\frac{2\pi i(k-1)(n-1)}{N_1}\right) \quad 1 \le n \le N_1. \quad (16)$$

We use this notation also for the right hand side, for example the DFT in the first variable reads

$$F_{k,j} = \sum_{n=1}^{N_1} f_{n,j} \exp\left(\frac{-2\pi i(k-1)(n-1)}{N_1}\right) \quad 1 \le k \le N_1.$$

To indicate the discrete Fourier transform in both variables, we write bars:

$$\bar{U}_{k,m} = \sum_{j=1}^{N_2} U_{k,j} \exp\left(\frac{-2\pi i(m-1)(j-1)}{N_2}\right) \quad 1 \le m \le N_2.$$

The following theorem states that the methodology for the discretized Laplace equation with periodic boundary conditions can also be applied to discretized homogeneous linear elastostatics.

Theorem 3 *For $1 \le k \le N_1$ and $1 \le m \le N_2$, but $km > 1$*

$$\bar{U}_{k,m} = \frac{d_{k,m}\bar{F}^u_{k,m} - b_{k,m}\bar{F}^v_{k,m}}{a_{k,m}d_{k,m} - b^2_{k,m}} h^2, \quad (17)$$

$$\bar{V}_{k,m} = \frac{a_{k,m}\bar{F}^v_{k,m} - b_{k,m}\bar{F}^u_{k,m}}{a_{k,m}d_{k,m} - b^2_{k,m}} h^2 \quad (18)$$

where

$$a_{k,m} = -4c - 2 + 2(c+1)\cos\frac{2\pi(k-1)}{N_1} + 2c\cos\frac{2\pi(m-1)}{N_2},$$
$$b_{k,m} = -\sin\frac{2\pi(k-1)}{N_1}\sin\frac{2\pi(m-1)}{N_2},$$
$$d_{k,m} = -4c - 2 + 2c\cos\frac{2\pi(k-1)}{N_1} + 2(c+1)\cos\frac{2\pi(m-1)}{N_2}.$$

Proof. Define

$$e_{k,n} \equiv \exp\left(\frac{2\pi i(k-1)(n-1)}{N_1}\right).$$

After a transform in the first variable and substituting (16) for n, $n+1$ and $n-1$ into (14) we get for fixed[1] n, $1 \le n \le N_1$

$$\frac{1}{N_1}\sum_{k=1}^{N_1} e_{k,n}\left(-4c - 2 + 2(c+1)\cos\frac{2\pi(k-1)}{N_1}\right)U_{k,j} + \frac{c}{N_1}\sum_{k=1}^{N_1} e_{k,n}\left(U_{k,j+1} + U_{k,j-1}\right) + \\ + \frac{1}{2iN_1}\sum_{k=1}^{N_1} e_{k,n}\sin\frac{2\pi(k-1)}{N_1}\left(-V_{j,k+1} + V_{j,k-1}\right) = \frac{h^2}{N_1}\sum_{k=1}^{N_1} e_{k,n}F^u_{k,j}$$

[1]Recall that index arithmetic is modulo grid size.

and

$$\frac{1}{N_1}\sum_{k=1}^{N_1} e_{k,n}\left(-4c - 2 + 2c\cos\frac{2\pi(k-1)}{N_1}\right)V_{k,j} + \frac{c+1}{N_1}\sum_{k=1}^{N_1} e_{k,n}\left(V_{k,j+1} + V_{k,j-1}\right) + \\ + \frac{1}{2iN_1}\sum_{k=1}^{N_1} e_{k,n}\sin\frac{2\pi(k-1)}{N_1}\left(-U_{j,k+1} + U_{j,k-1}\right) = \frac{h^2}{N_1}\sum_{k=1}^{N_1} e_{k,n}F^v_{k,j}.$$

By the independence of the Fourier modes, for fixed k and n:

$$\left(-4c - 2 + 2(c+1)\cos\frac{2\pi(k-1)}{N_1}\right)U_{k,j} + c\left(U_{k,j+1} + U_{k,j-1}\right) + \\ + \frac{1}{2i}\sin\frac{2\pi(k-1)}{N_1}\left(-V_{j,k+1} + V_{j,k-1}\right) = h^2F^u_{k,j}$$

and

$$\left(-4c - 2 + 2c\cos\frac{2\pi(k-1)}{N_1}\right)V_{k,j} + (c+1)\left(V_{k,j+1} + V_{k,j-1}\right) + \\ + \frac{1}{2i}\sin\frac{2\pi(k-1)}{N_1}\left(-U_{j,k+1} + U_{j,k-1}\right) = h^2F^v_{k,j}.$$

By the same argument, after a transform in the second variable, for fixed $1 \le k \le N_1$ and $1 \le m \le N_2$

$$h^2\bar{F}^u_{k,m} = -\sin\frac{2\pi(k-1)}{N_1}\sin\frac{2\pi(m-1)}{N_2}\bar{V}_{k,m} + \\ + \left(-4c - 2 + 2(c+1)\cos\frac{2\pi(k-1)}{N_1} + 2c\cos\frac{2\pi(m-1)}{N_2}\right)\bar{U}_{k,m} \quad (19)$$

$$h^2\bar{F}^v_{k,m} = -\sin\frac{2\pi(k-1)}{N_1}\sin\frac{2\pi(m-1)}{N_2}\bar{U}_{k,m} + \\ + \left(-4c - 2 + 2c\cos\frac{2\pi(k-1)}{N_1} + 2(c+1)\cos\frac{2\pi(m-1)}{N_2}\right)\bar{V}_{k,m} \quad (20)$$

The inversion of (19) and (20) for $\bar{U}$, $\bar{V}$ with k, m such that $km > 1$ yields just the formulas in the theorem. □

Remark 5.1 *For $k = m = 1$, the derivation of the system for $\bar{F}^u$ and $\bar{F}^v$ in the theorem remains valid, but in this case $a = b = d = 0$. By (19) and (20), the solution of the 2D elastostatic equations with periodic boundary conditions exists only if $\bar{F}^u(1,1) = \bar{F}^v(1,1) = 0$. In this case, the solution is not unique. We can choose arbitrary values for $\bar{U}(1,1)$ and $\bar{V}(1,1)$. In the implementation we set them to zero. This means that the finite difference operator with periodic boundary conditions is invertible on the subspace of grid vector fields (g^u, g^v) whose first and second components each sum to zero.*

5.2 Periodic Boundary Conditions in 3D

In 3 space dimensions, the same technique also yields a fast elastostatic solver for periodic boundary conditions. We discretize the equations of elastostatics (2) as follows.

$$(1+c)u_{n+1,j,\ell} + u_{n,j+1,\ell} + u_{n,j,\ell+1} - (4+2c)u_{n,j,\ell} + (1+c)u_{n-1,j,\ell} + u_{n,j-1,\ell} + u_{n,j,\ell-1} \\ + \frac{c}{4}v_{n+1,j+1,\ell} + \frac{c}{4}v_{n-1,j-1,\ell} - \frac{c}{4}v_{n-1,j+1,\ell} - \frac{c}{4}v_{n+1,j-1,\ell} \\ + \frac{c}{4}w_{n+1,j,\ell+1} + \frac{c}{4}w_{n-1,j,\ell-1} - \frac{c}{4}w_{n-1,j,\ell+1} - \frac{c}{4}w_{n+1,j,\ell-1} = f^u_{n,j,\ell},$$

$$v_{n+1,j,\ell} + (1+c)v_{n,j+1,\ell} + v_{n,j,\ell+1} - (4+2c)v_{n,j,\ell} + v_{n-1,j,\ell} + (1+c)v_{n,j-1,\ell} + v_{n,j,\ell-1}$$
$$+ \frac{c}{4}u_{n+1,j+1,\ell} + \frac{c}{4}u_{n-1,j-1,\ell} - \frac{c}{4}u_{n-1,j+1,\ell} - \frac{c}{4}u_{n+1,j-1,\ell}$$
$$+ \frac{c}{4}w_{n,j+1,\ell+1} + \frac{c}{4}w_{n,j-1,\ell-1} - \frac{c}{4}w_{n,j+1,\ell-1} - \frac{c}{4}w_{n,j-1,\ell+1} = f^v_{n,j,\ell},$$

$$w_{n+1,j,\ell} + w_{n,j+1,\ell} + (1+c)w_{n,j,\ell+1} - (4+2c)w_{n,j,\ell} + w_{n-1,j,\ell} + w_{n,j-1,\ell} + (1+c)w_{n,j,\ell-1}$$
$$+ \frac{c}{4}u_{n+1,j,\ell+1} + \frac{c}{4}u_{n-1,j,\ell-1} - \frac{c}{4}u_{n+1,j,\ell-1} - \frac{c}{4}u_{n-1,j,\ell+1}$$
$$+ \frac{c}{4}v_{n,j+1,\ell+1} + \frac{c}{4}v_{n,j-1,\ell-1} - \frac{c}{4}v_{n,j+1,\ell-1} - \frac{c}{4}v_{n,j-1,\ell+1} = f^w_{n,j,\ell}.$$

Theorem 4 *For $1 \le k \le N_1$, $1 \le m \le N_2$ and $1 \le p \le N_3$, but $kmp > 1$*

$$\begin{pmatrix} a_{k,m,p} & b_{k,m,p} & g_{k,m,p} \\ b_{k,m,p} & d_{k,m,p} & e_{k,m,p} \\ g_{k,m,p} & e_{k,m,p} & f_{k,m,p} \end{pmatrix} \begin{pmatrix} \hat{U}_{k,m,p} \\ \hat{V}_{k,m,p} \\ \hat{W}_{k,m,p} \end{pmatrix} = h^2 \begin{pmatrix} \hat{F}^u_{k,m,p} \\ \hat{F}^v_{k,m,p} \\ \hat{F}^w_{k,m,p} \end{pmatrix},$$

where

$$a_{k,m,p} = -(4+2c) + 2(1+c)\cos\frac{2\pi(k-1)}{N_1} + 2\cos\frac{2\pi(m-1)}{N_2} + 2\cos\frac{2\pi(p-1)}{N_3},$$
$$b_{k,m,p} = -c\sin\frac{2\pi(k-1)}{N_1}\sin\frac{2\pi(m-1)}{N_2},$$
$$g_{k,m,p} = -c\sin\frac{2\pi(k-1)}{N_1}\sin\frac{2\pi(p-1)}{N_3},$$
$$d_{k,m,p} = -(4+2c) + 2\cos\frac{2\pi(k-1)}{N_1} + 2(1+c)\cos\frac{2\pi(m-1)}{N_2} + 2\cos\frac{2\pi(p-1)}{N_3},$$
$$e_{k,m,p} = -c\sin\frac{2\pi(m-1)}{N_2}\sin\frac{2\pi(p-1)}{N_3},$$
$$f_{k,m,p} = -(4+2c) + 2\cos\frac{2\pi(k-1)}{N_1} + 2\cos\frac{2\pi(m-1)}{N_2} + 2(1+c)\frac{2\pi(p-1)}{N_3}.$$

Proof. The proof is completely analogue to 2D. Hats denote 3D FFTs, e.g. $\hat{W}$ is the 3D Fourier transform of the displacement w in the third spacial variable z. □

For completeness, we note that (here short $a = a_{k,m,p}, \ldots, f = f_{k,m,p}$)

$$A^{-1} = \frac{1}{\det(A)} \begin{pmatrix} df - e^2 & -bf + ge & be - gd \\ -bf + ge & af - g^2 & -ae + bg \\ be - gd & -ae + bg & ad - b^2 \end{pmatrix},$$

and $\det(A) = adf + 2bge - ae^2 - fb^2 - dg^2$. Whenever $kmp > 1$, we have $\det(A) \neq 0$. For $kmp = 1$ the derivations for the theorem still hold, but all coefficients in A are zero. In that case we require $\hat{F}^u_{1,1,1} = \hat{F}^v_{1,1,1} = \hat{F}^w_{1,1,1} = 0$ and in that case choose $\hat{U}_{1,1,1} = \hat{V}_{1,1,1} = \hat{W}_{1,1,1} = 0$.

5.3 Normal boundary conditions in 2D

Neither Dirichlet nor Neumann boundary conditions can be solved by reflection because of the different nature of the second order centered differences for first and second derivatives. The symmetric differences for ∂_{xx} and ∂_{yy} keep the same sign under reflection, while the antisymmetric differences for ∂_{xy} change signs under reflection.

To avoid this difficulty, we consider "normal" boundary conditions.

$$\begin{aligned} u(0,y) = u(N_1h,y) &= 0, \quad y \in [0, N_2h], \\ v_x(0,y) = v_x(N_1h,y) &= 0, \quad y \in (0, N_2h), \\ v(x,0) = v(x,N_2h) &= 0, \quad x \in [0, N_1h], \\ u_y(x,0) = u_y(x,N_2h) &= 0, \quad x \in (0, N_1h). \end{aligned}$$

Using Schwarztrauber's discretization of the normal boundary condition (c.f. §3) and a symmetry–based implementation of Dirichlet boundary conditions results in $(N_1+1) \times (N_2+1)$ discrete variables each for u, and v. The system of linear equations is reducible. We find a total of five blocks, two in u variables on the two vertical sides with Dirichlet boundary conditions, two in v variables on the two horizontal sides with Dirichlet boundary conditions, and one for all the interior variables and variables with Neumann boundary conditions. The subsystems on the Dirichlet boundaries all four have solution zero as expected.

To take advantage of the fast periodic solver, we use antisymmetric reflections for u and f^u in x and v and f^v in y, and symmetric reflections for u and f^u in y and v and f^v in x, with extension by zero at all four corners for both f^u and f^v.

Theorem 5 *The solution of the discretization of homogeneous linear elastostatics in 2D with normal boundary conditions exists and is unique. The extension $(\tilde{u}, \tilde{v})$ as described above solves the periodic system on $(2N_1) \times (2N_2)$ points with right hand side $(\tilde{f}^u, \tilde{f}^v)$.*

Proof. Solutions to the reflected system exist and are unique up to an additive constant each for $\tilde{u}$ and $\tilde{v}$ by Theorem 3 since $\sum \tilde{f}^u = \sum \tilde{f}^v = 0$. By symmetry of $\tilde{f}^u$ and $\tilde{f}^v$, preservation of symmetry under the DFT (c.f. §3.4 and §4.4) and symmetry properties of the $a_{k,m}$, $b_{k,m}$ and $d_{k,m}$, the solution $(\tilde{u}, \tilde{v})$ (choosing the solutions with $\hat{U}_{1,1,1} = 0$ and $\hat{V}_{1,1,1} = 0$) has the claimed form. Inspection shows that the appropriate restriction of the solution to the upper left quarter satisfies the difference equations and "normal" boundary conditions. □

The reorderings of the extensions are indicated symbolically below. Between sign changes and at the four corners, fill in zero. Between same size quantities, fill in appropriate boundary values.

2D

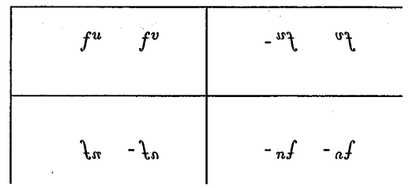

Remark 5.2 *Nonzero Dirichlet and Neumann boundary conditions have a similar interpretation in terms of the EJIIM as we showed for Laplace's equation.*

Remark 5.3 *The quadrupling of the domain can be avoided using an ansatz in sine and cosine series as outlined in §3.4 and §4.4.*

5.3.1 Example

To get an idea of what the benefits of the fast elastostatic solver can be, we implemented the matrices of the discretization of linear elastostatics in 2D with normal boundary conditions. Figure 3 visualizes linear and cubic growth (dots) as well as the solution times of Matlab's "slash" operator (a direct method, crosses) applied to these sparse matricesand the fast elastostatic solver (circles) in a loglog plot against the size of the linear system of equations. Note that the fast solver does not require the matrices! On the horizontal axis, we show the number of variables for "slash",$N = 2(N_1+1)(N_2+1)$. Due to the reflections the fast solver performs two FFTs and two inverse FFTs of length $4N_1N_2$. We see cubic behavior for the direct solver, and $N \log N$ behavior for the fast solver. We have chosen values of N so that the dependence of the performance of the FFT on the prime decomposition of N shows. For large N, we could not perform the direct solve in memory (without swapping), and consequently show only the data for the fast solver for such N.

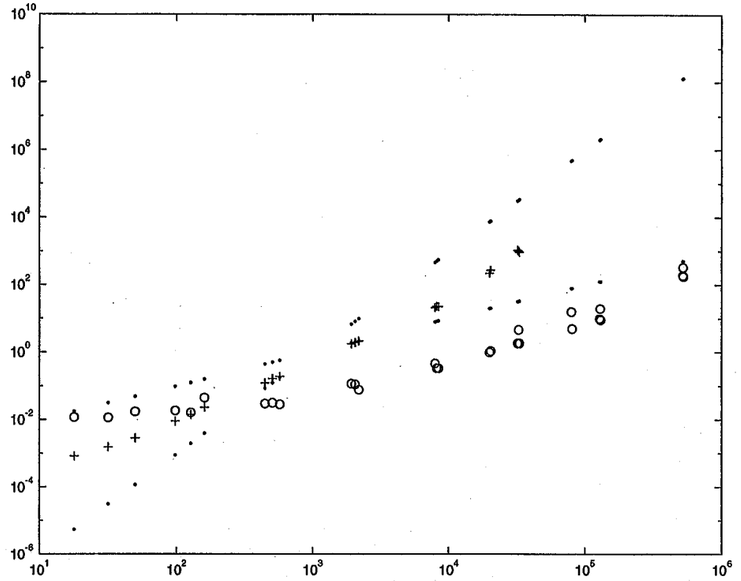

Figure 3: *Solution times of the fast elastostatic solver (circles, up to $N = 261121$) and Matlab's "slash" operator (a direct method, crosses, only up to $N = 16641$) in a loglog plot against the size of the linear system of N equations solved by the direct method. We plot dots at $N/1024$ and $(N/1024)^3$ to compare with linear and cubic growth.*

Remark 5.4 *This fast solver is used in [7] to solve problems on arbitrary domains with essential, natural and rigid punch boundary conditions.*

5.4 Normal boundary conditions in 3D

In 3D, "normal" boundary conditions are

$$\begin{aligned}
u(0,y,z) = u(N_1h_1,y,z) = 0, &\quad y \in [0,N_2h_2], z \in [0,N_3h_3],\\
v_x(0,y,z) = v_x(N_1h_1,y,z) = 0, &\quad y \in (0,N_2h_2), z \in (0,N_3h_3),\\
w_x(0,y,z) = w_x(N_1h_1,y,z) = 0, &\quad y \in (0,N_2h_2), z \in (0,N_3h_3),\\
v(x,0,z) = v(x,N_2h_2,z) = 0, &\quad x \in [0,N_1h_1], z \in [0,N_3h_3],\\
u_y(x,0,z) = u_y(x,N_2h_2,z) = 0, &\quad x \in (0,N_1h_1), z \in (0,N_3h_3),\\
w_y(x,0,z) = w_y(x,N_2h_2,z) = 0, &\quad x \in (0,N_1h_1), z \in (0,N_3h_3),\\
w(x,y,0) = w(x,y,N_3h_3) = 0, &\quad x \in [0,N_1h_1], y \in [0,N_2h_2],\\
u_z(x,y,0) = u_z(x,y,N_3h_3) = 0, &\quad x \in (0,N_1h_1), y \in (0,N_2h_2),\\
v_z(x,y,0) = v_z(x,y,N_3h_3) = 0, &\quad x \in (0,N_1h_1), y \in (0,N_2h_2).
\end{aligned}$$

Using Schwarztrauber's discretization of the normal boundary condition (c.f. §3) and a symmetry–based implementation of Dirichlet boundary conditions results in $(N_1+1)\times(N_2+1)\times(N_3+1)$ discrete variables each for u, v and w. As in the 2D case, the system of linear equations is reducible. We find a total of seven blocks, two in u variables on two opposite vertical faces with Dirichlet boundary conditions, two in v variables on the other two vertical faces with Dirichlet boundary conditions, two in w variables on the two horizontal faces with Dirichlet boundary conditions and one for all the interior variables and Neumann boundary variables. The subsystems on the Dirichlet boundaries all six have solution zero as expected.

To take advantage of the fast periodic solver, we use antisymmetric reflections for u and f^u in x, v and f^v in y and w and f^w in z, and symmetric reflections for u and f^u in y and z, v and f^v in x and z and v and f^w in x and y, with extension by zero at the twelve edges and eight corners for f^u, f^v and f^w.

Theorem 6 *The solution of the discretization of homogeneous linear elastostatics with normal boundary conditions exists and is unique. The extension $(\tilde{u},\tilde{v},\tilde{w})$ as described above solves the periodic system on $(2N_1)\times(2N_2)\times(2N_3)$ points with right hand side $(\tilde{f}^u,\tilde{f}^v,\tilde{f}^w)$.*

Proof. Solutions to the reflected system exist and are unique up to an additive constant each for $\tilde{u}$, $\tilde{v}$ and $\tilde{w}$ by Theorem 4 since $\sum\tilde{f}^u = \sum\tilde{f}^v = \sum\tilde{f}^w = 0$. By symmetry of $\tilde{f}^u$, $\tilde{f}^v$ and $\tilde{f}^w$, preservation of symmetry under the DFT (c.f. §3.4 and §4.4) and symmetry properties of the $a_{k,m,p}$, $b_{k,m,p}$, $d_{k,m,p}$, $e_{k,m,p}$, $f_{k,m,p}$ and $g_{k,m,p}$, the solution $(\tilde{u},\tilde{v},\tilde{w})$ (choosing the solutions with $\hat{U}=0$, $\hat{V}=0$ and $\hat{W}=0$) has the claimed form. Inspection shows that the appropriate restriction of the solution to the upper left quarter satisfies the difference equations and "normal" boundary conditions. □

We indicate symbolically the reflections needed for the "normal" boundary conditions in 3D. As before, the f^* and their reflections indicate a 3-dimensional array of values of the right hand side of the respective the elastostatic equation. Typewritten `f` indicates reflection in the third index.

3D

$f^u \quad f^v \quad f^w$	$-\mathtt{f}^u \quad \mathtt{f}^v \quad \mathtt{f}^w$
$\mathtt{f}^u \quad \mathtt{f}^v \quad -\mathtt{f}^w$	$-\mathtt{f}^u \quad \mathtt{f}^u \quad -\mathtt{f}^w$

$f_u \quad -f_v \quad f_w$	$-f_{nu} \quad -f_{av} \quad mf_w$
$\mathtt{f}_u \quad -\mathtt{f}_v \quad \mathtt{f}_w$	$-\mathtt{f}_{nu} \quad -\mathtt{f}_{av} \quad m\mathtt{f}_w$

There are also two layers of boundary values (in f^u and f^v) and a layer of zeros (in the f^w slots) below the left and between the two volumes.

Remark 5.5 *The octupling of the domain can be avoided using an ansatz in sine and cosine series as outlined in §3.4 and §4.4.*

5.5 Displacement Boundary Conditions in 2D

The following "fast" solver for Dirichlet boundary conditions in 2 space dimansions is very similar to the treatment of Neumann boundary conditions via Schur complements in [5, 9] and earlier capacitance matrix methods [2], except that here the inverse in the Schur–formula is a pseudo inverse! The Dirichlet boundary value problem for a linear elastic body is:

$$\begin{aligned}
c\Delta u + \partial_{xx}u + \partial_{xy}v = \tilde{f}^u \text{ in } \Omega,\\
c\Delta v + \partial_{xy}u + \partial_{yy}v = \tilde{f}^v \text{ in } \Omega,\\
u = 0 \text{ on } \partial\Omega \cup \partial\Omega',\\
v = 0 \text{ on } \partial\Omega \cup \partial\Omega'.
\end{aligned}$$

Due to the nature of the finite differences for the ∂_{xy} term, so far a direct fast inverter for Dirichlet boundary conditions has eluded me. For now, I use an iterative procedure that could possibly be used in parallel with the EJIIM embedding by stacking. The idea is to embed the body in a periodic domain (see Figure 4) and to find the appropriate extension boundary that makes the extended u and v vanish on the extension of Ω. Precisely, the problem is to find u, v, and in addition boundary values for the right hand side f_u^b and f_v^b such that the partial differential equation with Dirichlet boundary conditions can be rewritten in terms of a

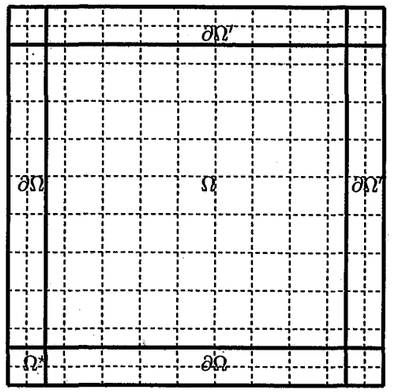

Figure 4: *The domain for the Dirichlet problem is Ω (bounded by inner fat lines). The discrete variables for the Dirichlet problem live on the 49 inner intersections. Ω is enlarged on the left and bottom to the rectangle with periodic boundary conditions. The two rectangles labeled $\partial\Omega'$ are periodically identified with the opposite rectangles, the three unlabeled squares are periodically identified with the bottom left square.*

partial differential equation with periodic boundary conditions

$$\begin{aligned}
c\Delta u + \partial_{xx}u + \partial_{xy}v &= \tilde{f}^u \text{ in } \Omega,\\
c\Delta v + \partial_{xy}u + \partial_{yy}v &= \tilde{f}^v \text{ in } \Omega,\\
c\Delta u + \partial_{xx}u + \partial_{xy}v - f_b^u &= 0 \text{ on } \partial\Omega,\\
c\Delta v + \partial_{xy}u + \partial_{yy}v - f_b^v &= 0 \text{ on } \partial\Omega,\\
c\Delta u + \partial_{xx}u + \partial_{xy}v - f_\star^u &= 0 \text{ at } \Omega^\star,\\
c\Delta v + \partial_{xy}u + \partial_{yy}v - f_\star^v &= 0 \text{ at } \Omega^\star,\\
u &= 0 \text{ on } \partial\Omega,\\
v &= 0 \text{ on } \partial\Omega,\\
u &= 0 \text{ at } \Omega^\star,\\
v &= 0 \text{ at } \Omega^\star.
\end{aligned}$$

A complication arises because the solution of the elastostatic equations with periodic boundary conditions on $\Omega \cup \partial\Omega \cup \Omega^\star$ exists only if each component of the right hand side integrates to zero. We ensure this by setting $f_\star^u = -\sum \tilde{f}^u - \sum f_b^u$ and $f_\star^v = -\sum \tilde{f}^v - \sum f_b^v$. In this case the solution is unique only up to two constants. Different from §5.1, we are not interested in the solution that sums to zero in each component, but in the unique u and v that vanish at $\Omega^\star$. The conditions that u and v vanish on $\Omega^\star \cup \partial\Omega$ determine f_b^u and f_b^v.

Numerically, we solve the following problem:

$$\begin{pmatrix} c\Delta_h^p + D_{xx}^p & D_{xy}^p & -E_b & 0\\ D_{xy}^p & c\Delta_h^p + D_{yy}^p & 0 & -E_b\\ R_b & 0 & 0 & 0\\ 0 & R_b & 0 & 0 \end{pmatrix} \begin{pmatrix} U\\ V\\ F_b^u\\ F_b^v \end{pmatrix} = \begin{pmatrix} EF^u\\ EF^v\\ 0\\ 0 \end{pmatrix}. \tag{21}$$

The superscript p indicates that the differential operators are discretized with periodic boundary conditions; R_b means the restriction of a grid function to values on the boundary (i.e. from the periodic domain to $\partial\Omega \cup \Omega^\star$); E_b is the extension (prolongation) from $\partial\Omega$ to $\partial\Omega \cup \Omega \cup \Omega^\star$ by zero in Ω, assigning $F_\star = -\sum F_b$ at $\Omega^\star$. Finally, E is the prolongation from Ω to $\Omega \cup \partial\Omega \cup \Omega^\star$ by zero in $\partial\Omega$, assigning $F_\star = -\sum F$ at $\Omega^\star$.

The reason for writing (21) is to take advantage of the fast solver for the periodic problem in a Schur–complement. Recall that if

$$\begin{pmatrix} A_{11} & A_{12}\\ A_{21} & A_{22} \end{pmatrix} \begin{pmatrix} U_1\\ U_2 \end{pmatrix} = \begin{pmatrix} F_1\\ F_2 \end{pmatrix}$$

and A_{11}^{-1} exists, then U_1 can be eliminated from the equations via $U_1 = A_{11}^{-1}(F_1 - A_{12}U_2)$. This elimination yields

$$(A_{22} - A_{21}A_{11}^{-1}A_{12})U_2 = F_2 - A_{21}A_{11}^{-1}F_1.$$

The main difficulty is that the difference matrix for the periodic problem, the upper left 2 by 2 block in (21), is not invertible. Since $\sum(EF^u) = 0$, $\sum(EF^v) = 0$, $\sum(E_bF_b^u) = 0$ and $\sum(E_bF_b^v) = 0$ for all F^u, F^v, F_b^u and F_b^v, it is clear that $\left(EF^u, EF^v\right)^T$ and $\left(E_bF_b^u, E_bF_b^v\right)^T$ are always in the range of the periodic finite difference operator

$$A = \begin{pmatrix} c\Delta_h^p + D_{xx}^p & D_{xy}^p\\ D_{xy}^p & c\Delta_h^p + D_{yy}^p \end{pmatrix}.$$

For any F in the range of A, $A^\dagger F$ indicates the vector $\left(U, V\right)^T$ that satisfies the periodic finite differences $A\left(U, V\right)^T = F$ with vanishing entries at Ω^*, $U^\star = 0$ and $V^\star = 0$. U and V can be found in $\mathcal{O}(n \ln n)$ by the technique in §5.1 and subtraction of $U^\star$, $V^\star$ from the solution found there. We rewrite (21) as

$$R_bU(F_b^u, F_b^v) = -R_bU(F^u, F^v), \tag{22}$$
$$R_bV(F_b^u, F_b^v) = -R_bV(F^u, F^v), \tag{23}$$

where

$$\begin{pmatrix} U(F^u, F^v)\\ V(F^u, F^v) \end{pmatrix} \equiv A^\dagger \begin{pmatrix} EF^u\\ EF^v \end{pmatrix}$$

and

$$\begin{pmatrix} U(F_b^u, F_b^v)\\ V(F_b^u, F_b^v) \end{pmatrix} \equiv A^\dagger \begin{pmatrix} E_bF_b^u\\ E_bF_b^v \end{pmatrix},$$

respectively.

We solve (22)–(23) for F_b^u, F_b^v via GMRES, a conjugate gradient method. An iterative method is needed because we do not explicitly know $A^\dagger$, but we can apply it in $\mathcal{O}(n \ln n)$.

Theorem 7 *There exists a unique solution $\{U, V, F_b^u, F_b^v\}$ of (21). Furthermore, the restriction of this solution to interior points solves the original discrete Dirichlet problem.*

Proof.

- **Existence:** Extend the (unique) solution to the discrete Dirichlet problem by zero on $\partial\Omega \cup \Omega^\star$ and calculate F_b^u, F_b^v, $F_\star^u$ and $F_\star^v$ via periodic finite differences. This explicit form shows that they are unique. It is a general property of periodic finite differences that the sum over the output vector vanishes, and hence $F_\star^u = -\sum F^u - \sum F_b^u$ and, $F_\star^v = -\sum F^v - \sum F_b^v$. But this means that the so-constructed $\{U, V, F_b^u, F_b^v\}$ satisfy (21).
- **Uniqueness:** Let (U, V, F_b^u, F_b^v) be any solution. Since the entries of both U and V are zero on the boundary by the third and fourth block rows in (21), by the prolongation by zero property of E_b the entries corresponding to the interior points solve the Dirichlet boundary value problem. Hence they are unique, and with them also F_b^u and F_b^v.

□

5.5.1 Example

To evaluate the performance of the solver for displacement boundary conditions we have implemented the matrices of the discretization of linear elastostatics in 2D with essential boundary conditions. The matrices were applied to grid functions u and v to obtain right hand sides f^u and f^v with known solutions. We used GMRES [3] to solve (22)—(23). In Table 1 we see results as the residue for zero initial guess is reduced by 10 orders of magnitude — the usual mode of using GMRES.

Table 1: *Performance of the Displacement solver for N grid points.*

N	Iterations	Flops	Flop Ratio, $N = 4^m$	Mflops	Seconds	Time Ratio
15^2	23	3.6e+06	—	1.9e+0	1.9	—
16^2	23	1.9e+06	—	8.6e−1	2.2	—
17^2	25	9.3e+06	—	4.6e+0	2.0	—
31^2	31	6.6e+07	—	1.9e+1	3.5	—
32^2	31	1.1e+07	5.8	3.5e+0	3.1	1.4
33^2	32	3.8e+07	—	1.1e+1	3.5	—
63^2	39	1.6e+08	—	2.3e+1	7.1	—
64^2	39	5.9e+07	5.4	8.6e+0	6.9	2.2
65^2	39	2.2e+08	—	2.9e+1	7.6	—
127^2	48	6.5e+09	—	1.1e+2	61	—
128^2	48	3.2e+08	5.4	1.2e+1	26	3.8
129^2	48	2.5e+09	—	6.8e+1	37	—
255^2	59	6.8e+09	—	4.5e+1	150	—
256^2	59	1.7e+09	5.3	1.1e+1	156	6.0
257^2	59	6.6e+10	—	1.3e+2	513	—
511^2	72	1.0e+11	—	8.1e+1	1234	—
512^2	72	8.7e+09	5.1	1.1e+1	809	5.2
513^2	72	3.7e+10	—	3.5e+1	862	—

The following points are noteworthy

- The GMRES iteration count grows very slowly as the mesh is refined.
- The number of floating point iterations needed depends strongly on the prime factors of the number of grid points due to the use of the FFT.
- The runtimes are less sensitive, because for "bad" prime factorizations the FFT uses the CPU more efficiently — at least for the "small" problems in the table.
- For powers of two, the optimal number of grid points, and due the almost constant iteration count, the flops (and runtimes) grow with $\mathcal{O}(N \ln N)$, just like the solver for periodic boundary conditions.

6 Conclusions

We have described the fast solution of Poisson problems on rectangular parallelepipeds in one, two and three space dimensions, and reduced the solution of Dirichlet and Neumann boundary value problems to the Poisson problem, using appropriate reflections.

Nonzero Dirichlet and Neumann boundary conditions were seen as special, grid-aligned cases of the jump conditions used in the Explicit Jump Immersed Interface Method.

The fast solver methodology for periodic boundary conditions carried over to the equations of homogeneous linear elastostatics in the approximation of plane stress and in three dimensions and is being used in [7] for general regions with essential, natural and rigid punch boundary conditions in 2D. For "normal" boundary conditions, reflection works in 2D and 3D and provides a simple proof of the regularity of the

matrix of the discretization. In 2D, the theoretical performance of $\mathcal{O}(N \ln N)$ was observed for the fast elastostatic solver for normal boundary conditions in an implementation.

For the Displacement boundary condition case, a "singular" Schur–complement technique was developed that avoids enlarging the domain, but requires several periodic solves. In this case, the number of iterations (solves with periodic boundary conditions) in GMRES required to reduce the residue by a fixed factor deteriorates only slightly as the mesh is refined.

7 Acknowledgments

I thank Dr. David Adalsteinsson and Dr. Alessandro Sarti for helpful discussions.

References

[1] B. L. Buzbee, F. W. Dorr, J. A. George, and G. H. Golub. The direct solution of the discrete Poisson equation on irregular regions. *SIAM J. Numer. Anal.*, 8(4):722—736, 1971.

[2] W. Proskurowski and O. Widlund. On the Numerical Solution of Helmholtz's Equation by the Capacitance Matrix Method. *Math. Comp.*, 30(135):433—468, 1976.

[3] Y. Saad and M. H. Schultz. GMRES: A generalized minimal residual Algorithm for solving nonsymmetric linear systems. *SIAM J. Sci. Statist. Comput.*, 7(3):856—869, 1986.

[4] P. N. Schwarztrauber. Fast Poisson Solvers. In G. H. Golub, editor, *Studies in Numerical Analysis*, volume 24, pages 319—370. MAA, 1984.

[5] A. Wiegmann. *The Explicit–Jump Immersed Interface Method and Interface Problems for Differential Equations.* PhD thesis, University of Washington, 1998.

[6] A. Wiegmann. The Explicit Jump Immersed Interface Method for homogeneous 2D Linear Elastostatics. In preparation, August 1999.

[7] A. Wiegmann. The Immersed Interface Method and Integral Formulas. Technical Report LBNL-43566, Lawrence Berkeley National Laboratory, MS 50A-1148, One Cyclotrone Rd, Berkeley CA 94720, June 1999.

[8] A. Wiegmann and K. P. Bube. The Explicit–Jump Immersed Interface Method: Finite Difference Methods for PDE with piecewise smooth solutions. To appear in *SIAM J. Numer. Anal.*

Ernest Orlando Lawrence Berkeley National Laboratory
One Cyclotron Road | Berkeley, California 94720

Prepared for the U.S. Department of Energy under Contract No. DE-AC03-76SF00098